

## Nano-Carrier for Accentuated Transdermal Drug Delivery

Vidhi Malika<sup>1</sup>, Kanchan Kohli<sup>2</sup>, Hema Chaudhary<sup>1\*</sup> and Vikash Kumar<sup>1</sup>

<sup>1</sup>P.D. Memorial College of Pharmacy, Sector-3A; Sarai Aurangabad, Bahadurgarh, India

<sup>2</sup>Department of Pharmacy, Jamia Hamdard, New Delhi, India

### Abstract

This research objective was to design a nano-carrier for Glibenclamide (GBD) by loading it in to nano-transfersomes to provide an accentuated transdermal drug delivery for Non-Insulin Dependent Diabetes Mellitus (NIDDM). The nano-transfersomes were prepared by sonication method and optimized using a statistically three-factor three-level Factorial Design (Box-Behnken design). A second order equation (polynomial) was originated and construct contour plots (2-D) for prediction the responses and characterized by various parameters (i.e. entrapment efficiency, vesicle shape & size, zeta potential, degree of deformability, permeation and skin irritation study). The skin permeation of optimized formulation (GNTs2) was found to be significantly higher (enhancement ratio is 10.44) than the drug in solution and also further confirmed by fluorescence microscopy using due i.e. Rhodamine B. Hence, drug loaded nano-transfersomes accentuates its transdermal flux and can be used as a nano-vehicle for NIDDM.

**Keywords:** Diabetic mellitus; Glibenclamide (GBD); Design; Nano-transfersomes; Transdermal delivery

### Introduction

Transdermal Drug Delivery System (TDDS) is an alternative to conventional delivery by lower the problems associated with the oral and parenteral administration of drugs. TDDS also bypasses the first pass metabolism effect that proved it suitability for low bioavailability drugs, to achieving a constant\controlled release of drug (especially for drugs having narrow therapeutic window) with minimize side effects attained by using variety of polymers (applied as a nano-carrier for microspheres, nanoparticles, gels etc. [1-5]). In TDDS route, drug molecules achieve a therapeutic amounts at their target site and skin application (limited due to the effective barrier properties of intact skin, primarily associated with the outermost layers of the epidermis, namely the stratum corneum) [6-10]. Also, there are numerous approaches have been adopted to overcome permeation problem associated with these routes, one such approach involves encapsulation of drug in a vesicular system i.e. a novel nano-carrier “nano-transfersomes” which is capable to improved transdermal delivery of drugs [11] which are ultra-deformable lipid supra-molecular aggregates. They are capable to penetrating across the intact mammalian skin when applied non-occlusive by using a surface active agent added in a proper ratio [sublytic concentrations provided certain degree of flexibility to the vesicle membrane]. NTs claimed to be able to squeeze through channels one-tenth their diameter, allowing them to spontaneously penetrate the stratum corneum due to the flexibility. They penetrate across the skin by osmotic gradient (driving force), which is caused by the difference in water content between the relatively dehydrated skin surface (~20% water) and the aqueous viable epidermis. A lipid suspension when applied to the skin is subjected to evaporation [in order to avoid dehydration], NTs penetrates to the deeper tissues and hence squeeze through stratum corneum lipid lamellar regions penetrating deeper to follow the osmotic gradient [12,13].

A mathematical and statistical technique response surface methodology (RSM-factorial design: central composite design, Box-Behnken design, and D-optimal design are the various types of designs) is available for modeling, optimization and analysis of problems influenced by several variables and evaluation of the relationship of a set of controlled experimental factors and observed results of the formulations [14,15]. Based on the principles of factorial designs; the methodology involves the use of Box-Behnken designs for generating

polynomial mathematical relationships and mapping the response over the experimental domain for selecting the optimum formulation. The design is independent quadratic designs which have the treatment combinations at the mid-points of the edges of the process space and at the center. For exploration, quadratic response construct a polynomial model which helping in optimizing of a process using small number of experimental domain [16-18].

Non-Insulin Dependent Diabetes Mellitus (NIDDM) is one of the most common diseases nowadays and characterized by moderate\ no reduction in  $\beta$  cell mass and generally low, normal or even high level of insulin in circulation, no  $\beta$  cell antibody is demonstrable and high degree of genetic disposition [19]. Glibenclamide (GBD: a BCS-II drug has low oral bioavailability & highly lipophilic) an oral hypoglycemic agent belonging to the category of sulphonylureas, on oral administration produces remarkable hypoglycemia, frequent GI side effects such as nausea, vomiting, heartburn, anorexia, increased appetite etc. and may even cause hyper-insulinemia, major risk factor for atherosclerosis. In order to counteract the shortcomings associated with oral therapy of GBD, transdermal delivery system can be developed, which in addition also provides an ease of termination of therapy on manifestation of serious side effects. GBD have already been proven to be effective in management of NIDDM on transdermal administration [20-23]. For this, the main aim of the study was to develop a novel nano formulation of the model drug i.e. GBD loaded nano-transfersomes for enhanced its transdermal delivery for NIDDM and its optimization using Box Behnken design.

### Materials and Methods

The model drug [GBD] was purchased from Suraksha Pharma Pvt Ltd. [Nagarjuna Nagar, Hyderabad]. Sodium Deoxy-cholate (SDC)

\*Corresponding author: Hema Chaudhary, P. D. Memorial College of Pharmacy, Sector-3A; Sarai Aurangabad, Bahadurgarh, India, Tel: 91-11-260-9688; E-mail: hema.manan@gmail.com

Received May 19, 2014; Accepted July 31, 2014; Published August 05, 2014

Citation: Malika V, Kohli K, Chaudhary H, Kumar V (2014) Nano-Carrier for Accentuated Transdermal Drug Delivery. J Develop Drugs 3: 121. doi:10.4172/2329-6631.1000121

Copyright: © 2014 Malika V, et al. This is an open-access article distributed under the terms of the Creative Commons Attribution License, which permits unrestricted use, distribution, and reproduction in any medium, provided the original author and source are credited.

and Rhodamine B were purchased from Control Drug House Pvt. Ltd, (New Delhi). Phospholipon 90G was a kind gift sample received from Lipoid GmbH (Ludwigshafen, Germany).

### Animals

The used Albino rats in the experiments were approved by the CPCSEA (Control and Supervision on Experiments on Animals, protocol approval no.: PDM/CPCSEA/RES/2012/10, PDM College of Pharmacy, India) committee.

### Preparation of GBD Loaded Nano-Transfersomes (GNTs)

Nano-transfersomes were prepared by sonication method using lipid (phospholipon 90G), surfactant (SDC) and ethanol (7% v/v) as hydrating medium. Precisely lipid, surfactant and model drug (GBD) mixture was dissolved in chloroform: methanol (1:1 v/v), then organic solvent was removed by rotary evaporation (Rotary Evaporator, Multitech Instrument Co. Pvt. Ltd. Delhi, India). The final traces of solvent were removed under vacuum overnight and deposited lipid film was hydrated with ethanol by rotation (60 rpm) for sixty minutes at room temperature. Resulting, vesicles were allowed to swell at room temperature (2 hr) to get LMLVs (large multi-lamellar vesicles) and probed by sonication (Hielscher Ultrasound technology (UP200S), Germany) for 10 to 30 min at 40W for prepare smaller vesicles. Furthermore, using polycarbonate membranes sandwich, sonicated vesicles were extruded (100 and 200 nm) [11].

### Experiments design

To explore the “quadratic response surface” and constructing a second order polynomial model using Design Matrix Expert i.e. three factor-three level Box-Behnken Design (Design Expert®, Version 8.07) comprising of experimental runs [22] was constructed and the non-linear computer generated quadratic model is defined as;

$$Y = b_0 + b_1X_1 + b_2X_2 + b_3X_3 + b_{12}X_1X_2 + b_{13}X_1X_3 + b_{23}X_2X_3 + b_{11}X_1^2 + b_{22}X_2^2 + b_{33}X_3^2$$

Where, Y is the dependent variable;  $b_0$  is the intercept;  $b_1$  to  $b_{33}$  are the regression coefficients from the experimental values of Y (dependent variables; entrapment efficiency ( $Y_1$ ), particle size ( $Y_2$ ) and transdermal flux ( $Y_3$ ); and  $X_1$ ,  $X_2$  and  $X_3$  ( $i=1, 2, \text{ or } 3$ ) independent variables (lipid to drug ratio ( $X_1$ ), lipid to surfactant ratio ( $X_2$ ) and sonication time ( $X_3$ ) represents the interaction and quadratic terms respectively. The dependent and independent variables with low, medium & high levels are illustrated (Table 1). The amount of dependent variable's ( $X_1$ =ratio of lipid to surfactant;  $X_2$ =weight of lipid to surfactant and  $X_3$ =sonication time) were used to prepared different batches of the drug loaded nano-transfersomes (GNTs) and their experimental responses ( $Y_1$ =entrapment efficiency;  $Y_2$ =particle size and  $Y_3$ =transdermal flux) are summarized in Table 1.

### Characterization of GNTs formulations

**Entrapment efficiency:** By ultra-centrifuged (14000 rpm) nano-transfersosomal suspension for 30 min. After that supernatant was diluted with methanolic HCl (0.01M), measured the absorbance (UV-Vis spectrophotometer (Jasco, V-630, Japan)) at 229 nm and entrapment efficiency calculated using formula as;

$$EE = \frac{[W_T - W_F]}{W_T} \times 100$$

Where, EE=entrapment efficiency;  $W_T$ =total amount of the drug in nano-transfersosomal suspensions;

$W_F$ =free amount of the drug.

**Vesicle size and zeta potential:** Particle size and zeta potential were measured by zeta sizer (Zeta nano series Z590, Malvern instruments). The system was used in auto measuring mode. The Polydispersibility Index (PI), a measure of homogeneity, was also determined by the same

| Factor   |             | Level used (Coded) |              |                                 |                                  |   |
|--|-------------|--------------------|--------------|---------------------------------|----------------------------------|---|
| Independent Variables  |             | Low (-1)           | Medium (0)   | High (+1)                       |                                  |   |
| $X_1$ = Lipid: drug (w/w)  |             | 21.36              | 26.70        | 32.40                           |                                  |   |
| $X_2$ = Lipid: Surfactant (w/w)  |             | 4.50               | 5.00         | 5.50                            |                                  |   |
| $X_3$ = Sonication time (min)  |             | 10.00              | 20.00        | 30.00                           |                                  |   |
| Dependent Variables = $Y_1$ (Entrapment Efficiency (%)), $Y_2$ (Particle size (nm)) and $Y_3$ (Transdermal flux ( $\mu\text{g}/\text{cm}^2/\text{hr}$ )) |             |                    |              |                                 |                                  |   |
| Design Results   |             |                    |              |                                 |                                  |   |
| Code   | $X_1$ (w/w) | $X_2$ (w/w)        | $X_3$ (min.) | $Y_1$ (%)<br>mean $\pm$ SD, n=3 | $Y_2$ (nm)<br>mean $\pm$ SD, n=3 | $Y_3$ ( $\mu\text{g}/\text{cm}^2/\text{hr}$ )<br>mean $\pm$ SD, n=3 |
| GNTs1  | 0           | 0                  | 0            | 69.10 $\pm$ 0.74                | 145.24 $\pm$ 3.48                | 53.39 $\pm$ 4.76  |
| GNTs2  | 0           | 0                  | 0            | 68.80 $\pm$ 0.56                | 142.24 $\pm$ 1.89                | 54.10 $\pm$ 3.63  |
| GNTs3  | +1          | +1                 | 0            | 59.96 $\pm$ 1.21                | 180.06 $\pm$ 5.56                | 36.65 $\pm$ 5.30  |
| GNTs4  | -1          | 0                  | +1           | 48.95 $\pm$ 1.23                | 156.15 $\pm$ 4.98                | 40.10 $\pm$ 3.81  |
| GNTs5  | 0           | 0                  | 0            | 68.90 $\pm$ 1.67                | 152.76 $\pm$ 3.80                | 53.40 $\pm$ 4.76  |
| GNTs6  | +1          | 0                  | +1           | 51.18 $\pm$ 2.56                | 166.58 $\pm$ 1.24                | 46.04 $\pm$ 2.48  |
| GNTs7  | 0           | +1                 | -1           | 86.88 $\pm$ 1.33                | 184.67 $\pm$ 3.43                | 42.78 $\pm$ 5.44  |
| GNTs8  | -1          | 0                  | -1           | 50.40 $\pm$ 0.75                | 158.32 $\pm$ 5.60                | 47.30 $\pm$ 7.20  |
| GNTs9  | 0           | -1                 | +1           | 72.68 $\pm$ 2.23                | 151.33 $\pm$ 4.69                | 48.52 $\pm$ 5.09  |
| GNTs10   | +1          | -1                 | 0            | 42.60 $\pm$ 1.32                | 140.04 $\pm$ 2.35                | 41.57 $\pm$ 9.36  |
| GNTs11   | 0           | 0                  | 0            | 69.10 $\pm$ 0.98                | 142.31 $\pm$ 1.36                | 53.39 $\pm$ 4.76  |
| GNTs12   | 0           | 0                  | 0            | 68.80 $\pm$ 3.34                | 147.68 $\pm$ 3.50                | 54.10 $\pm$ 3.63  |
| GNTs13   | +1          | 0                  | -1           | 51.17 $\pm$ 2.35                | 170.24 $\pm$ 4.21                | 36.56 $\pm$ 5.49  |
| GNTs14   | 0           | -1                 | -1           | 74.61 $\pm$ 1.13                | 175.09 $\pm$ 1.25                | 41.40 $\pm$ 3.21  |
| GNTs15   | -1          | +1                 | 0            | 54.33 $\pm$ 0.87                | 160.78 $\pm$ 2.12                | 39.94 $\pm$ 4.27  |
| GNTs16   | 0           | +1                 | +1           | 86.20 $\pm$ 4.39                | 191.23 $\pm$ 3.22                | 38.31 $\pm$ 5.04  |
| GNTs17   | -1          | -1                 | 0            | 45.59 $\pm$ 0.87                | 154.33 $\pm$ 3.89                | 43.50 $\pm$ 4.58  |

$Y_1$ =entrapment efficiency (%);  $Y_2$ =particle size (nm) and  $Y_3$ =transdermal flux  $\mu\text{g}/\text{cm}^2/\text{hr}$

Table 1: Box-Behnken design variables and results.

instrument. A small value of PI (<0.2) is an indication of homogeneity of vesicular population.

**Vesicle shape and morphology:** For morphological characterization, transmission electron microscopic (TEM) studies using Phosphotungstic Acid (PTA) as a negative stain were performed (Moragagni 268D FEI, The Netherlands). A drop of the sample was placed on a carbon-coated copper grid to leave a thin film on the grid, drop of the staining solution (PTA (1%) was added to the film, and the excess of the solution was drained off with a filter paper. The grid was allowed to thoroughly dry in air, and samples were viewed under a transmission electron microscope (Olympus, DX31, and Japan).

**Elasticity of vesicles:** The elasticity of DNTs was determined by nano-transfersomal suspension was extruded through filter membrane (pore diameter 100 and 200 nm, using a stainless steel filter holder) applying a pressure of 2.5 bar using extrusion method. The quantity of suspension extruded was measured and particle size after extrusion was measured using Zeta Sizer (Zeta Nano series Z590, Malvern Instruments) [24-26]. The elasticity value of vesicles was calculated by formula;

$$\text{Elasticity} = J \times (r_v / r_p)^2$$

Where, J=amount of suspension extruded in 5 minutes;  $r_v$ =vesicle size;  $r_p$ =pore diameter

### Drug release and permeation profile

The abdominal and dorsal skin of sacrificed rat was removed using scalpel and scissors, wrapped in aluminium foil and stored at a temperature (-20°C). On the day of experiment, skin was thawed, then hairs were removed at room temperature and subcutaneous fat was removed by cotton soaked in isopropyl alcohol [27]. Thus prepared skin was cut into pieces according to the area of diffusion cell and *ex vivo* permeation profile of GBD from nano-transfersomes was done [28,29]. The receptor was filled with phosphate buffer: ethanol [6:4] (pH-7.4) and the prepared skin was mounted over it, with stratum corneum facing donor compartment. The donor compartment was then clamped on the receptor compartment using springs and filled with nano-transfersomal suspension. The receptor medium was continuously stirred (200 rpm) using magnetic stirrer and a constant temperature of  $37 \pm 2^\circ\text{C}$  was maintained throughout the studies. Aliquots [0.5 ml] were drawn at intervals of 0.5, 1, 2, 3, 4, 6, 8, 10, 12, 16, 20 and 24 hr and were replaced by the same volume of receptor medium. The samples were suitably diluted using methanolic HCl (0.01 M) and analyzed spectrophotometer at 229 nm. The cumulative amount permeated was plotted against time, and the slope of the linear portion of the plot was estimated as the steady state flux [30]. The permeability coefficient and diffusion coefficient were calculated using following formulas:

$$K_p = J_{ss} / C_d$$

Where,  $K_p$ =permeability coefficient;  $J_{ss}$ =steady-state flux;  $C_d$ =concentration of drug in donor compartment.

### Histopathological study

The skin was cut into small circular pieces and two pieces of the skin were taken in two different studies of 6 hrs and 24 hrs respectively. The formulation was applied on the stratum corneum of the skin and the treated skin was left undisturbed for specified periods. The control and treated skins were stored in neutral buffered saline (10%). After specified periods, the skins were removed from neutral buffered saline, dehydrated in graded concentrations of ethanol, immersed in xylene, and then embedded in paraffin. The five micrometer thick sections of

skin were cut using microtome and mounted on slide using commercial baker's mounting fluid. The paraffin was removed by warming the slide gently, until wax melted, and then washed with xylene followed by washing with absolute alcohol and water. The sections were stained with hemato-xylins eosin to determine gross histopathology. The slides were analyzed by optical microscope at 400X magnification [31].

### Fluorescence microscopy

Drug loaded nano-transfersomes (GNTs) with Rhodamine B (provide the fluorescence labeling) was prepared as described method in section 2.2. The vesicle-skin interaction studied to confirm the better skin penetration using two rats (Wistar rats (weighing 120-160 g)); first rat received the application of aqueous solution of Rhodamine B alone (control) and applied GNTs with Rhodamine B on the dorsal skin surface of second one. After six hour of application, the rats (skin was removed, cut into small pieces and fixed) were sacrificed and examined under a fluorescence microscope [11,32].

### Skin irritation study

For the skin irritation study, the dorsal side of rat (weighed around 230-250 gm) present hairs were removed using scalpel and the optimized formulation was applied. Any sign of irritation i.e. erythema/redness for a period of 24 hrs was observed.

### Stability studies

The Optimized NTs formulation was packed in amber colored glass bottle and stored at  $5 \pm 3^\circ\text{C}$  (storage condition) and  $25 \pm 2^\circ\text{C}/75 \pm 5\% \text{RH}$  (for accelerated stability study) [33] for a period of three months. The formulation was periodically evaluated for entrapment efficiency and visual changes. The shelf life of the GNTs2 was obtained using software *Sigma Plot, version 12.5*.

## Result and Discussion

### Entrapment efficiency (EE)

The percentage fraction of total drug incorporated (EE) into the NTs was obtained in range between  $45.59 \pm 0.87$  to  $86.88 \pm 1.33$  (Table 1). The entrapment efficiency usually increases with increase in lipid to surfactant ratio (higher EE of GNTs7) further increase in the surfactant concentration showed a decrease in the entrapment efficiency. The initial increment in drug entrapment in the presence of low concentrations of surfactant may be due to the growth in vesicle size owing to the incorporation of more amount of drug. The entrapment efficiency was found to decrease with an increase in concentration of surfactant (>15 % w/w). This is due to the fact that at lower concentration (<15% w/w) the surfactant molecules get associated with the phospholipid bilayer. Above a certain concentration, some surfactant molecules lead to increased permeability of the vesicle membrane by generating pores thereby making the membrane leaky, and hence resulting in decreased entrapment efficiency. Also, when the concentration of surfactant in the bi-layer is increased beyond its critical micellar concentration (beyond 15% w/w), mixed micelles with lower entrapment efficiency were formed [34,35].

### Vesicle Size and Zeta Potential

The particle size and zeta potential of the nano-transfersomal formulation (DNTs) was found to be in range  $140.04 \pm 2.35$  to  $191.23 \pm 3.22$  nm and  $-29.7 \pm 1.03$  to  $-18.9 \pm 1.56$  (Tables 1 and 2) respectively. Particle size increases with increase in lipid to surfactant ratio ( $X_1$ ) and vice-versa with sonication time ( $X_2$ ). The greater stability to GNTs due to more negative value of zeta potential and also poly-dispersibility index

(PDI<1) [36,37] indicated narrow size distribution and homogeneity of the dispersion.

### Degree of deformability

The elasticity of nano-transfersomes vesicles is most considerable parameter of nano-transfersomal formulations because this parameter differentiates it from other vesicular carriers and helping it to pass through narrow pores. Deformability index increased significantly with increase in the lipid concentration and beyond a certain concentration it decreases which may be attributed to rigidization effect observed at higher concentration of lipid (Table 2). It was found to be increase with increase in concentration of surfactant (up-to 15% w/w) but when concentration is further increased (beyond 15%), degree of deformability decrease was observed (owing to the formation of mixed micelle, which bears rigid membrane). Due to high flexibility, drug loaded nano-transfersomes pass through much smaller pores than their diameter and risk of skin rupture completely minimizing.

### Drug release study

The amount of drug permeated determined the amount of drug

which is available for absorption, so cumulative drug release, and permeation coefficient obtained from nano-transfersomal formulation at the end of 24hr (Figure 1). The value is substantially higher than that which is typically driven by transdermal concentration gradients. The higher permeation rate from nano-transfersomes is due to the capability of lipid to spontaneously penetrate across the skin due to transdermal hydration gradient. Xerophobia [11], affinity to avoid dry environs, causes the surface of skin dehydration resist which results drug transport from the dry skin surface to better hydrated skin.

### Data fitting

All responses ( $Y_1$ ,  $Y_2$  and  $Y_3$  from prepared seventeen formulations) were fitted to first order, second order and quadratic models designs. Resulting, quadratic was the best-fitted model and the proportional values of  $R^2$ , SD, and %CV are given along with each response regression equation with statistically significant ( $p<0.05$ ) coefficients.

### Equation analysis

A positive and negative value indicates; the effect that favors the

| Formulation Code | Zeta potential (mV) mean $\pm$ SD, n=3 | PDI mean $\pm$ SD, n=3 | Extruded volume (ml) | Degree of deformability |
|------------------|--|------------------------|----------------------|-------------------------|
| GNTs1            | -28.9 $\pm$ 2.31                       | 0.212 $\pm$ 2.30       | 7.8 $\pm$ 1.30       | 15.37                   |
| GNTs2            | -29.7 $\pm$ 1.03                       | 0.174 $\pm$ 1.45       | 8.1 $\pm$ 0.90       | 15.70                   |
| GNTs3            | -25.0 $\pm$ -0.70                      | 0.167 $\pm$ 3.12       | 5.3 $\pm$ 2.67       | 16.07                   |
| GNTs4            | -22.3 $\pm$ -0.35                      | 0.204 $\pm$ 0.98       | 8.0 $\pm$ 1.11       | 17.10                   |
| GNTs5            | -22.3 $\pm$ -0.35                      | 0.204 $\pm$ 0.98       | 7.6 $\pm$ 2.93       | 15.23                   |
| GNTs6            | -20.5 $\pm$ 2.34                       | 0.182 $\pm$ 3.48       | 8.6 $\pm$ 1.09       | 21.62                   |
| GNTs7            | -27.7 $\pm$ -1.20                      | 0.194 $\pm$ 4.38       | 4.8 $\pm$ 1.87       | 15.79                   |
| GNTs8            | -21.6 $\pm$ 1.80                       | 0.135 $\pm$ 0.98       | 7.8 $\pm$ 1.15       | 18.04                   |
| GNTs9            | -26.7 $\pm$ -1.50                      | 0.179 $\pm$ 1.68       | 5.8 $\pm$ 1.89       | 12.23                   |
| GNTs10           | -20.7 $\pm$ 1.04                       | 0.134 $\pm$ 1.89       | 6.5 $\pm$ 3.62       | 11.01                   |
| GNTs11           | -27.9 $\pm$ 1.31                       | 0.200 $\pm$ 4.25       | 7.9 $\pm$ 1.30       | 15.08                   |
| GNTs12           | -28.9 $\pm$ -0.31                      | 0.177 $\pm$ 1.23       | 7.6 $\pm$ 2.93       | 14.97                   |
| GNTs13           | -23.3 $\pm$ 1.32                       | 0.198 $\pm$ 3.64       | 8.6 $\pm$ 1.09       | 22.05                   |
| GNTs14           | -19.8 $\pm$ 1.69                       | 0.190 $\pm$ 1.65       | 8.5 $\pm$ 0.33       | 24.94                   |
| GNTs15           | -28.1 $\pm$ -0.70                      | 0.159 $\pm$ 4.78       | 5.2 $\pm$ 1.87       | 13.00                   |
| GNTs16           | -22.3 $\pm$ 0.89                       | 0.186 $\pm$ 1.88       | 3.7 $\pm$ 1.87       | 22.80                   |
| GNTs17           | -24.2 $\pm$ -1.36                      | 0.147 $\pm$ 3.26       | 7.3 $\pm$ 1.11       | 10.66                   |

Table 2: Data of all formulations.

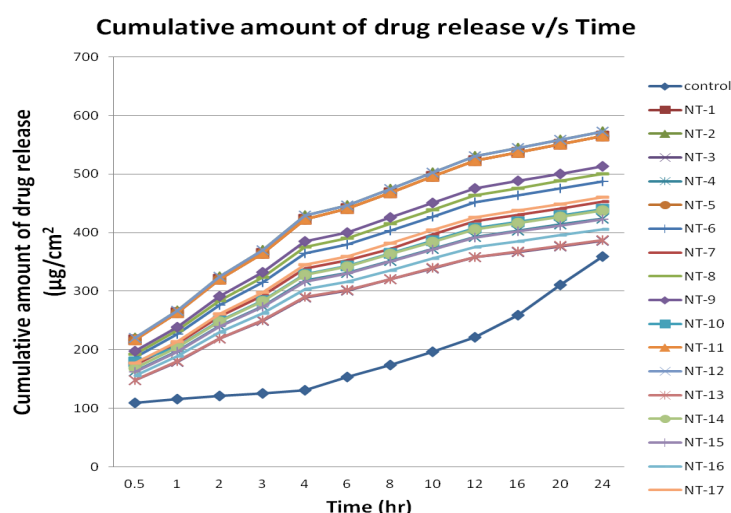
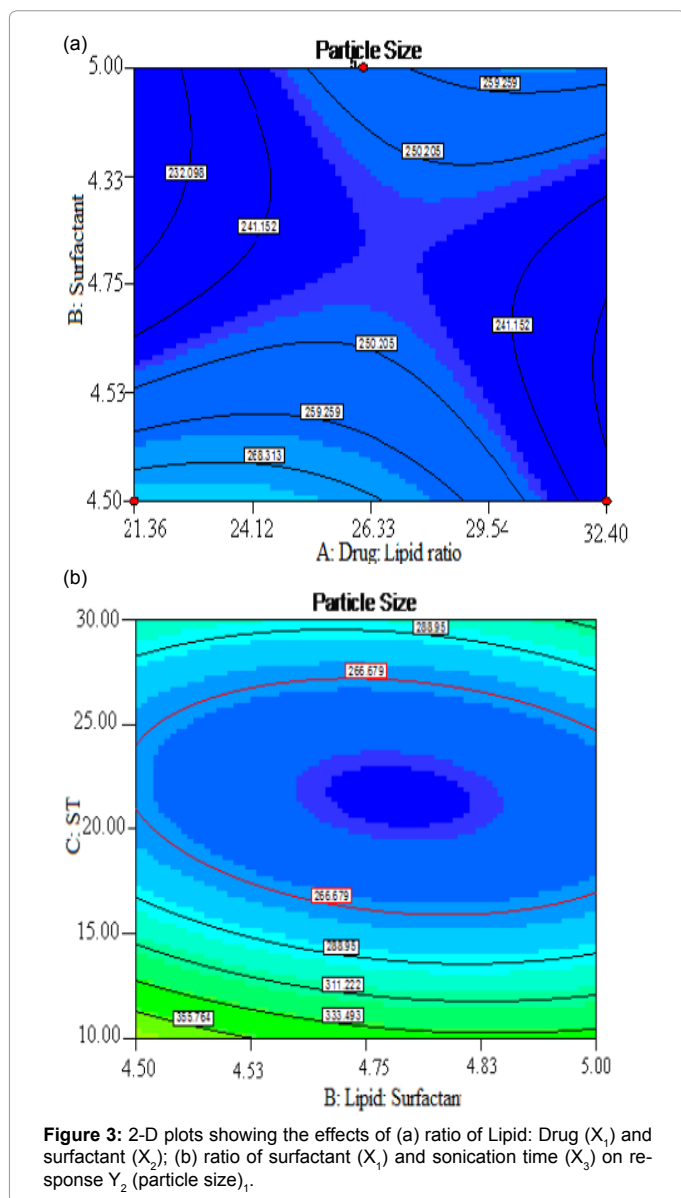


Figure 1: The cumulative drug releases of all formulations at the end of 24 hr.





are helpful in studying effects of two factors at one time on the response. For validation of RSM results, established high values of  $R^2$  for all the three responses). The  $R^2$  value for responses  $Y_1$ ,  $Y_2$  and  $Y_3$  was found to be 0.9999, 0.9999 and 0.9974, respectively. Thus, a low error magnitude significant proved the high predictive ability of the RSM.

### Optimization

The optimum formulation of GBD loaded nano-transfersomes was selected based on the criteria of attaining maximum value of percentage EE and transdermal flux, minimizing vesicle size by applying Design Expert prediction method. Upon "trading off" various variables and comprehensive evaluation of feasibility search and exhaustive grid search, GNTs2 was fulfilled the requisite of optimum formulation.

### Optimized GNTs2

The optimized formulation was characterized by vesicle shape (morphology), vesicle size and size distribution, entrapment efficiency (%EE), transdermal flux, zeta potential, drug release and kinetics, permeation studies, vesicle skin interaction (fluorescence microscopy

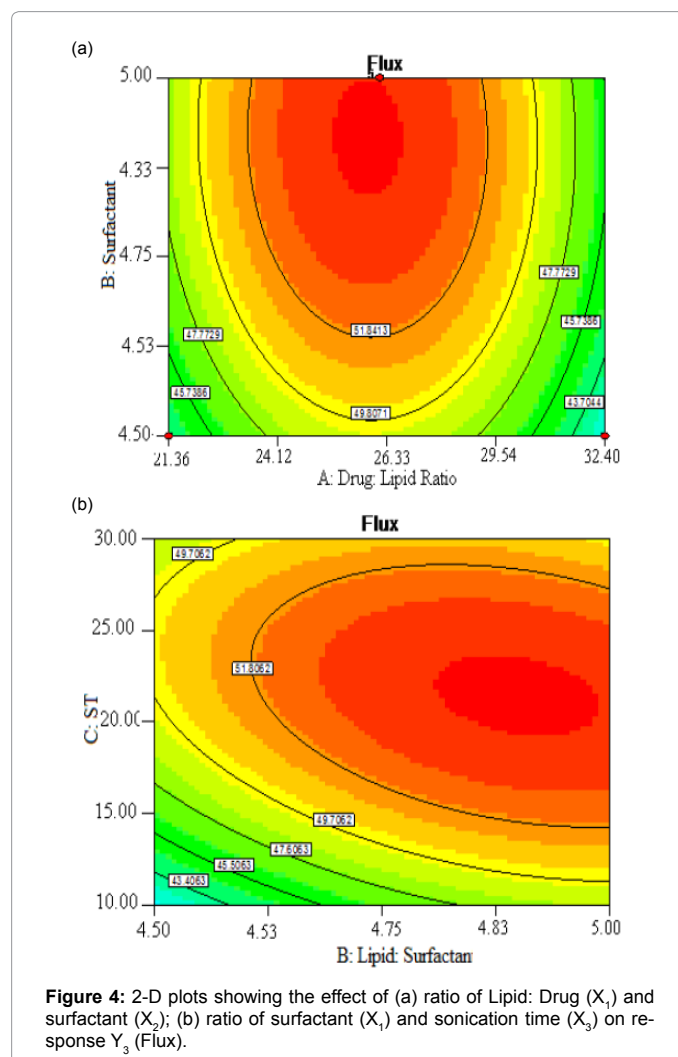
and skin irritation study. GNTs2 showed high stability of the formulation due to high %EE:  $68.80 \pm 0.56$ ; vesicle size:  $142.24 \pm 1.89$  nm; transdermal flux:  $54.10 \pm 3.63$   $\mu\text{g}/\text{cm}^2/\text{hr}$  and -29.7 value of zeta potential. The small poly-dispersibility index (PI=0.174) value proved narrow size distribution and dispersion homogeneity in the optimized formulation.

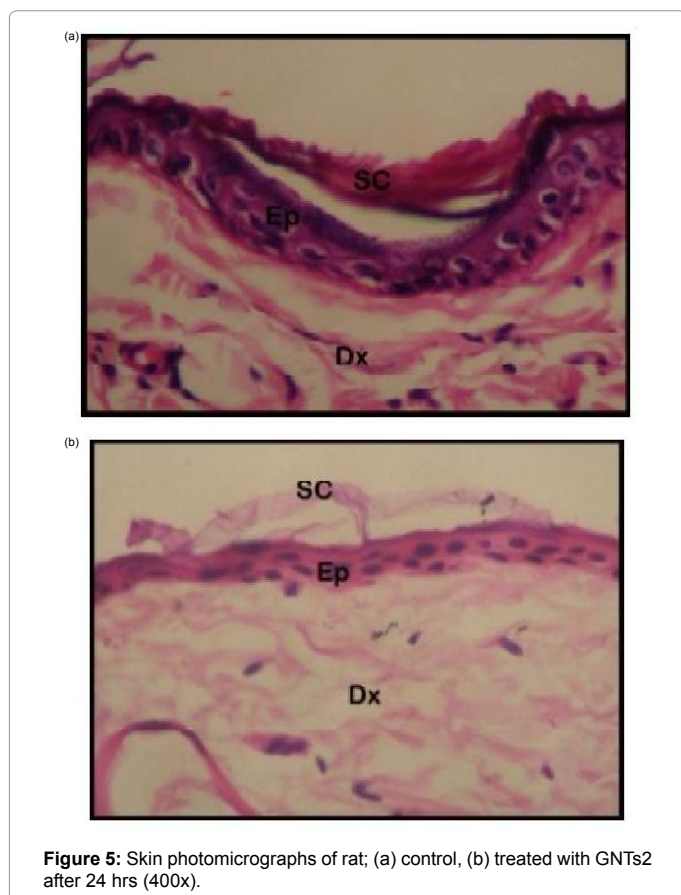
### Drug release

GNTs transdermal flux is  $54.10 \pm 3.63$   $\mu\text{g}/\text{cm}^2/\text{hr}$ , where as it is only  $5.18 \pm 2.66$   $\mu\text{g}/\text{cm}^2/\text{hr}$  for the control (enhancement ratio=10.44), indicating much higher penetration capacity of drug entrapped in nano-transfersomes compared to the drug in solution. This can be attributed to better partitioning of drug entrapped in nano-transfersomes compared to drug in solution and high elasticity of the nano-transfersomal membrane. Moreover, at time 0.5 hr, the Cumulative Drug Release (CDR) of control ( $108.86 \pm 1.44$   $\mu\text{g}/\text{cm}^2$ ) and GNTs2 ( $219.86 \pm 6.38$   $\mu\text{g}/\text{cm}^2$ ) showing that nano-transfersomal formulation will show a quicker onset of action. CDR higher in GNTs2 at 0.5 hr is due to burst effect and higher flux obtained with the nano-transfersomes may be attributed to increase in thermodynamic activity, increased skin vehicle partitioning of drug, alteration in the barrier properties of the skin and elasticity of vesicle membrane [35].

### Skin histopathology

The high power photomicrograph and fluorescent micrographs of





untreated rat skin (control); showed dermis (Dx), epidermis (Ep) and stratum corneum (SC) (Figures 5 and 6). The corneal layer is quite well formed with the layers compacted. The epidermis is three to four cells thick with normal stratification. The skin photomicrograph treated with optimized formulation (GNTs2) for 6 hrs, the corneal layer is thinner and partly separated from the underlying epidermis which shows thinning of two to three layers, indicating the disruption of stratum corneum by nano-transfersomes. In case of skin treated for 24 hrs. (Figure 5), the corneal layer is mostly lost with some fragments of poorly stained corneal cells seen on the underlying epidermis and the epidermis here is also reduced in thickness with loss of basal layer cells, which shows further disruption of lipid bi-layer.

### Fluorescence microscopy

The skin treated with rhodamine B dye solution i.e. control and skin treated with dye loaded GNTs2; In the control skin, stratum corneum is intact and the dye almost remained confined to the stratum corneum with a minimal penetration [by the virtue of the dye lipophilicity] [38]. Whereas, in case of skin treated with dye loaded GNTs2, the stratum corneum was found to be disrupted, and nano-transfersomes appearing as clusters of particles showing fluorescence can be seen in the epidermis and in the deeper layers. Therefore, it can be concluded that nano-transfersomes penetrate across the skin by disrupting the stratum corneum, while remaining intact themselves, and reaches the deeper layers of the skin.

### Release kinetics

The *ex vivo* diffusion data was applied to zero order, first order, Higuchi kinetics and Korsmeyer Peppas models to find out the release

kinetics of the GNTs2. The mathematical evaluation of order of release correlation regression was determined to know the order of drug release. The highest value of regression coefficient has been obtained for zero order kinetic models ( $R^2=0.9862$ ), indicating drug release from GNTs2 follows zero order kinetics, i.e. drug release first increases with time and then becomes constant. The value of  $n$  for the drug release was found to be 0.253, showing that *Quasi Fickian* drug release mechanism has been followed by the optimized formulation (GNTs2).

### Skin irritation study

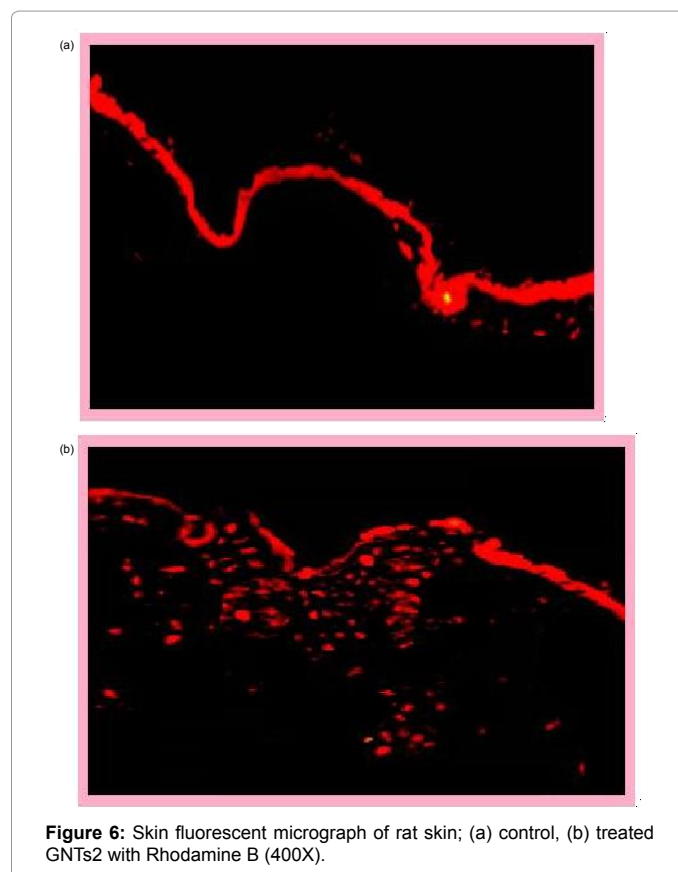
A primary skin irritation test was conducted with rats to determine the potential of GNTs2 to produce irritation after a single topical application. There was no sign of irritation [no redness/erythema] was observed after 24 hrs of application of the optimized formulation. Therefore, the optimized formulation is safe on topical application.

### Stability studies

Optimized formulation (GNTs2) showed no significant changes in visual, entrapment efficiency and drug content at interval of 15, 30, 60 and 90 days (three months period), under both the conditions (accelerated and long term storage).

### Conclusion

In order to counteract the shortcomings associated with oral therapy of Glibenclamide (GBD), transdermal delivery system has been developed, which in addition also provides an ease of termination of therapy on manifestation of serious side effects. The present study was an attempt to enhance transdermal delivery of GBD, by loading it in novel approach (nano-transfersomes). The histopathology study showed loosening and disruption of stratum corneum indicated



penetration of GNTs2 across stratum corneum. The GNTs2 (flux was 10.44 more than control) has much higher penetration and its drug release followed zero order kinetics. During accelerated and long term storage, GNTs2 showed no significant changes, shelf life was 368.110 days and skin irritation study proved its safety for topical use.

## Conflict Of Interest

The author's confirmed that there is no conflict of content.

## Acknowledgment

The author's grateful to Suraksha Pharma Pvt Ltd, Nagarjuna Nagar [Hyderabad] and Lipoid GmbH, Ludwigshafen (Germany) was provided the kind gift sample of model drug and Phospholipon 90G to carry out the research work. The authors wish to thanks Management of PDMREA, PDM Group of Institution (PDM College of Pharmacy), Sarai Aurangabad, Bahadurgarh (Haryana) for providing financial support and facilities.

## References

- Aminabhavi TM, Nadagouda MN, Joshi SD, More UA (2014) Guar gum as platform for the oral controlled release of therapeutics. See comment in PubMed Commons below *Expert Opin Drug Deliv* 11: 753-766.
- Chaturvedi K, Ganguly K, Kulkarni AR, Kulkarni VH, Nadagouda MN, et al. (2011) Cyclodextrin-based siRNA delivery nanocarriers: a state-of-the-art review. See comment in PubMed Commons below *Expert Opin Drug Deliv* 8: 1455-1468.
- Rudzinski WE, Aminabhavi TM (2010) Chitosan as a carrier for targeted delivery of small interfering RNA. See comment in PubMed Commons below *Int J Pharm* 399: 1-11.
- Chaturvedi K, Ganguly K, Nadagouda MN, Aminabhavi TM (2013) Polymeric hydrogels for oral insulin delivery. See comment in PubMed Commons below *J Control Release* 165: 129-138.
- Mundargi RC, Rangaswamy V, Aminabhavi TM (2011) Poly(N-vinylcaprolactam-co-methacrylic acid) hydrogel microparticles for oral insulin delivery. See comment in PubMed Commons below *J Microencapsul* 28: 384-394.
- Vyas SP, Khar RK (2002) *Controlled Drug Delivery: Concepts and Advances*, 1st edition, Vallabh Prakashan, New Delhi.
- Bouwstra JA, Honeywell-Nguyen PL, Gooris GS, Ponc M (2003) Structure of the skin barrier and its modulation by vesicular formulations. See comment in PubMed Commons below *Prog Lipid Res* 42: 1-36.
- Alexander A, Dwivedi S, Ajazuddin, Giri TK, Saraf S, et al. (2012) Approaches for breaking the barriers of drug permeation through transdermal drug delivery. See comment in PubMed Commons below *J Control Release* 164: 26-40.
- Cevc G (1996) Transfersomes, liposomes and other lipid suspensions on the skin: permeation enhancement, vesicle penetration, and transdermal drug delivery. See comment in PubMed Commons below *Crit Rev Ther Drug Carrier Syst* 13: 257-388.
- Lopez RF, Seto JE, Blankschtein D, Langer R (2011) Enhancing the transdermal delivery of rigid nanoparticles using the simultaneous application of ultrasound and sodium lauryl sulfate. See comment in PubMed Commons below *Biomaterials* 32: 933-941.
- Chaudhary H, Kohli K, Kumar V (2013) Nano-transfersomes as a novel carrier for transdermal delivery. See comment in PubMed Commons below *Int J Pharm* 454: 367-380.
- Benson HA (2006) Transfersomes for transdermal drug delivery. See comment in PubMed Commons below *Expert Opin Drug Deliv* 3: 727-737.
- Schatzlein A, Cevc G (1995) Characterization, metabolism, and novel biological applications. Champaign, AOCS Press, 191-209.
- Agyralides GG, Dallas PP, Rekkas DM (2004) Development and in vitro evaluation of furosemide transdermal formulations using experimental design techniques. See comment in PubMed Commons below *Int J Pharm* 281: 35-43.
- Giannakou SS, Dallas PP, Rekkas DM, Choulis NH (1995) Development and in vitro evaluation of nitrendipine transdermal formulations using experimental design techniques. *International Journal of Pharmaceutics* 125: 7-15.
- Chaudhary H, Kohli K, Amin S, Rathee P, Kumar V (2011) Optimization and formulation design of gels of Diclofenac and Curcumin for transdermal drug delivery by Box-Behnken statistical design. See comment in PubMed Commons below *J Pharm Sci* 100: 580-593.
- Chaudhary H, Rohilla A, Rathee P, Kumar V (2013) Optimization and formulation design of carbopol loaded Piroxicam gel using novel penetration enhancers. See comment in PubMed Commons below *Int J Biol Macromol* 55: 246-253.
- Gupta A, Gaud RS, Ganga S (2010) Development of Buccal adhesive formulations using in-situ formation of inter-polymer complex and optimization using box-benhken design. *International Journal of Advances Pharmaceutical Sciences* 1: 86-95.
- Trotta M, Peira E, Carlotti ME, Gallarate M (2004) Deformable liposomes for dermal administration of methotrexate. See comment in PubMed Commons below *Int J Pharm* 270: 119-125.
- Ali A, Trehan A, Ullah Z, Aqil M, Sultana Y (2011) Matrix type transdermal therapeutic systems of glibenclamide: Formulation, ex vivo and in vivo characterization. See comment in PubMed Commons below *Drug Discov Ther* 5: 53-59.
- Mishra MK, Ray D, Barik BB (2009) Microcapsules and transdermal patch: a comparative approach for improved delivery of antidiabetic drug. See comment in PubMed Commons below *AAPS PharmSciTech* 10: 928-934.
- Mutalik S, Udupa N (2004) Glibenclamide transdermal patches: physicochemical, pharmacodynamic, and pharmacokinetic evaluations. See comment in PubMed Commons below *J Pharm Sci* 93: 1577-1594.
- Mutalik S, Udupa N (2005) Formulation development, in vitro and in vivo evaluation of membrane controlled transdermal systems of glibenclamide. See comment in PubMed Commons below *J Pharm Pharm Sci* 8: 26-38.
- Sheo DM, Shweta A, Ram CD, Ghanshyam M, Girish K, et al. (2010) Transfersomes-a novel vesicular carrier for enhanced transdermal delivery of Stavudine: Development, characterization and performance evaluation. *Journal of Science and Speculations Research* 1: 30-36.
- Jain S, Jain P, Umamaheshwari RB, Jain NK (2003) Transfersomes--a novel vesicular carrier for enhanced transdermal delivery: development, characterization, and performance evaluation. See comment in PubMed Commons below *Drug Dev Ind Pharm* 29: 1013-1026.
- Hiruta Y, Hattori Y, Kawano K, Obata Y, Maitani Y (2006) Novel ultra-deformable vesicles entrapped with bleomycin and enhanced to penetrate rat skin. See comment in PubMed Commons below *J Control Release* 113: 146-154.
- Zheng WS, Fang XQ, Wang LL, Zhang YJ (2012) Preparation and quality assessment of itraconazole transfersomes. See comment in PubMed Commons below *Int J Pharm* 436: 291-298.
- Vinod KR, Anbazhagan S, Sunil MK, Sandhya S, Banji D, et al. (2013) Developing ultra deformable vesicular transportation of a bioactive alkaloid in pursuit of vitiligo therapy. *Asian Pacific Journal of Tropical Disease* 2: 301-306.
- Malakar J, Sen SO, Nayak AK, Sen KK (2012) Formulation, optimization and evaluation of transfersosomal gel for transdermal insulin delivery. See comment in PubMed Commons below *Saudi Pharm J* 20: 355-363.
- Jain A, Ghosh B, Nayak S, Soni V (2009) A study of transdermal delivery of Glibenclamide using Iontophoresis. *International Journal of Health Research* 2: 85-87.
- Singh HP, Utreja P, Tiwary AK, Jain S (2009) Elastic liposomal formulation for sustained delivery of colchicine: in vitro characterization and in vivo evaluation of anti-gout activity. See comment in PubMed Commons below *AAPS J* 11: 54-64.
- Aggarwal N, Goindi S (2012) Preparation and evaluation of antifungal efficacy of griseofulvin loaded deformable membrane vesicles in optimized guinea pig model of *Microsporum canis*-dermatophytosis. See comment in PubMed Commons below *Int J Pharm* 437: 277-287.
- ICH Harmonised Tripartite Guideline Q1A [R2] (2003) International conference on harmonisation of technical requirements for registration of pharmaceuticals for human use: stability testing of new drug substances and products. 1-18.
- Ahad A, Aqil M, Kohli K, Sultana Y, Mujeeb M, et al. (2012) Formulation and optimization of nanotransfersomes using experimental design technique for accentuated transdermal delivery of valsartan. See comment in PubMed Commons below *Nanomedicine* 8: 237-249.
- Mishra D, Garg M, Dubey V, Jain S, Jain NK (2007) Elastic liposomes mediated transdermal delivery of an anti-hypertensive agent: propranolol hydrochloride. See comment in PubMed Commons below *J Pharm Sci* 96: 145-150.
- Bavarsad N, Fazly Bazzaz BS, Khamesipour A, Jaafari MR (2012) Colloidal, in vitro and in vivo anti-leishmanial properties of transfersomes containing paromomycin sulfate in susceptible BALB/c mice. See comment in PubMed Commons below *Acta Trop* 124: 33-41.



37. Shah M, Pathak K (2010) Development and statistical optimization of solid lipid nanoparticles of simvastatin by using 2(3) full-factorial design. See comment in PubMed Commons below *AAPS PharmSciTech* 11: 489-496.
38. Vult von Steyern F, Josefsson JO, Tägerud S (1996) Rhodamine B, a fluorescent probe for acidic organelles in denervated skeletal muscle. See comment in PubMed Commons below *J Histochem Cytochem* 44: 267-274.